V_n harmonics at 200 GeV Au +Au collisions

By: Edwin Augustin

Nyack High School

November 16, 2011

Acknowledgements

I thank my mentor Dr. Paul Sorensen for giving me guidance and reassurance for the duration of his experiments. I thank his friends, Dr. Navneet Pruthi and Dr. Michael Mitrovski, for helping me in Dr. Sorensen's stead while he was away. I thank Ms. Mary-Beth Foisy, Mrs. Kirsten Kleinman, and Ms. Deidre O'Hagan for supporting me during my work in the Authentic Science Research Program.

Abstract

Physicists believe that the beginning of the universe was created with the Big Bang. The quark-gluon plasma is a state of matter in which the elementary particles, quarks and gluons, “melt” together to form a hot, dense state of matter. Little is understood about its properties. The collisions in the Relativistic Heavy-Ion Collider at Brookhaven National Laboratory reproduce quark-gluon plasma and the early universe a few microseconds after the Big Bang. This study implemented Fourier transform in an attempt to identify the mean-free-path of particles within the quark-gluon plasma, which could lead to a better understanding of its viscosity. The mean-free-path was found to indicate that the quark-gluon plasma is viscous, although further analysis is necessary to quantify this property.

Table of Contents

List of Figures ……. pg. 2

Introduction …… pg. 3

Statement of Purpose ……. pg. 6

Methodology …… pg. 7

Results …….. pg. 10

Discussion ……. pg. 17

References …….. pg. 18

List of Figures

Figure 1 …… pg. 3

Figure 2 …… pg. 7

Figure 3 …… pg. 8

Figure 4 …… pg. 10

Figure 5 …… pg. 10

Figure 6 …… pg. 10

Figure 7 …… pg. 11

Figure 8 …… pg. 11

Figure 9 …… pg. 12

Figure 10 …….. pg. 12

Figure 11 …….. pg. 12

Figure 12 …….. pg. 13

Figure 13 …….. pg. 13

Figure 14 …….. pg. 14

Figure 15 …….. pg. 14

Figure 16 …….. pg. 15

Figure 17 …….. pg. 16

Introduction

The universe has evolved in the thoughts of mankind from a obscure concept to topic of mystery. Physicists today believe that the universe as we know it today was created by the Big Bang, which is thought to have been an explosion triggering the formation of the modern universe. Very little is known about the early universe, such as what it was comprised of and what it was during the fractions of a second after the Big Bang. Models of the early universe indicate that, microseconds after the Big Bang, it was extremely hot and dense. The state of matter during this time is referred to as the quark-gluon plasma (QGP). The QGP was first created officially at the Relativistic Heavy-Ion Collider (RHIC) at Brookhaven National Laboratory in 2005 (Trafton, 2010). At RHIC, the QGP is usually created through collisions of gold nuclei (Au + Au) at energies of 200 GeV. During each of these collisions, hundreds of particles are formed; in essence as a hot, dense soup of quarks and gluons similar to the state of matter microseconds after the Big Bang. By studying the particles created during these collisions and the tracks made – a better understanding of the properties of QGP can be accomplished.

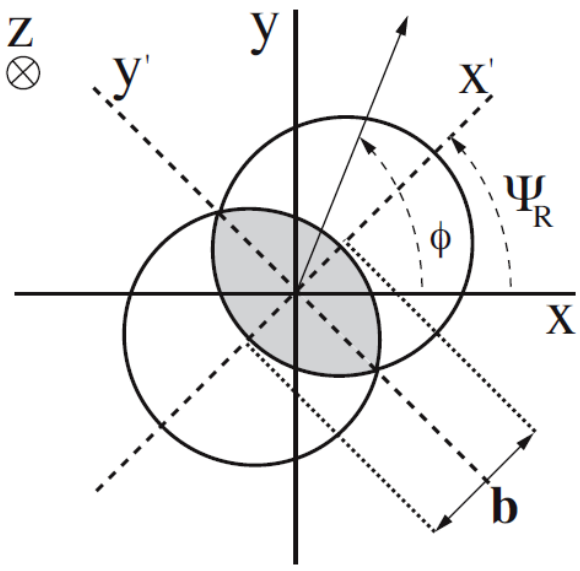

Figure 1: The azimuthal plane with respect to the reaction plane. (Bilandzic, Snellings, and Voloshin, 2011)

Viscosity is a very important concept in the area of fluid dynamics. It is a measure of a fluid's resistance to flow as well as how well momentum is transferred within the fluid. An understanding of the viscosity of the QGP is important in defining the behavior of QGP. Unlike

ordinary fluids, a QGP's degrees of freedom are represented by elementary particles. Quarks and their interactions are governed by the strong nuclear force instead of the electromagnetic force. Jacak and Steinburg conjectured that the QGP is a perfect fluid, in other words, a fluid with no viscosity (Jacak and Steinburg, 2010). During particle collisions, the nuclei overlap to form an elliptical region as shown in Fig. 1. Experiments have shown that during particle collisions, particles are not emitted at random angles, but at a direction that depends on the initial geometry of the collision. This directional dependency is called anisotropy and pressure gradients of the system serve as the indicator of anisotropy.

The detectors at RHIC can only give information about the momentum, energy, and charge of the particle, which means that information of the position of the particles is lost. The Fourier transform can be used to transfer the system from momentum space to coordinate space. According to the Heisenberg Uncertainty principle, as the accuracy of a measurement of a particle's momentum goes up, much of the information about the initial position of the particle becomes inaccurate. The Fourier transform is a tool to reduce these inaccuracies by using the pressure gradients and pressure maximums to determine the momentum distribution to determine the position of the particles before they fly out of the system.

The Fourier transform uses the Fourier series, which is a power series that allows one to interpret any graph as several terms of a cosine function. The series is represented by the formula $N(\varphi) \alpha 1+2V_1\cos(\varphi) +2V_2\cos(2\varphi) + 2V_3\cos(3\varphi)+\ldots$ where N represents the number of particles in the system emitted at the azimuthal angle, φ represents the azimuthal angle of the particles in the system with respect to the longitudinal axis (see Fig. 1), and V_n represent the nth harmonic value. The first harmonic in the series, V_1, represents directed flow and if the value is negative, it indicates that the particles are emerging back-to-back. And if positive, it indicates that the

particles are emerging in the same hemisphere. The second harmonic, V_2, reflects the shape of the initial ellipse, and is thus an indicator of momentum-space anisotropy. If the collision is head-on, the second harmonic should not vary much from the third, fourth and higher harmonics. The actual V_n values are solved for using a two-particle azimuthal correlation $\langle\cos[n(\varphi_1 - \varphi_2)]\rangle = \langle V_n^2\rangle + \delta_n$ (Bilandzic, Snellings, and Voloshin, 2011), and the use of Gaussian fits for the projections of V_n^2 vs. $\Delta\eta$, where $\Delta\eta$ is the pseudo-rapidity difference which represents the angle of two particles relative to the beam axis. In this equation, δ_n, represents the non-flow correlation caused by Bose-Einstein correlations and jet-scattering, which can create biased results, since it is unrelated to the initial geometry.

Statement of Purpose

Viscosity of the QGP cannot be directly measured. In addition, there is a limit to how accurately the detectors of RHIC can function. The accuracy of the detectors is reflected by the number of terms included in the Fourier series: the more accuracy, the more terms. After considering the number of terms the the detectors of RHIC can handle, the extent of the Fourier series is determined by observing what harmonics drop off to zero. This information reflects the probing scale of the system and can be used to determine the value of the mean-free-path (l_{mfp}) of the particles. The mean-free-path is the average path traveled by particles in the system without interacting with each other, and is related to viscosity; the smaller the mean-free-path, the less viscous the system. This study looked at the higher order harmonics of the Fourier cosine series of a two-particle correlation, in attempt to define conditions of the QGP; specifically to quantify the length of the mean-free-path. Data from the collisions of high centrality (i.e., more head-on), was analyze. The harmonic values were expected to be closely related to each other with higher centrality to indicate the extremely low viscosity of the system.

Methodology

At the very beginning of the project, data recording the particles detected from approximately 16 million Au+Au collisions at 200 GeV was collected from the STAR detector in RHIC. The data was recorded as a graph of Δη vs. centrality bins, where Δη is the pseudo-rapidity difference. Pseudo-rapidity relates to the angles between two particles' path on the longitudinal axis (see Figure 2). The centrality bins are ranges in the percent most central or "head on" collisions out of the total number of collisions starting with bin 0 being 80-100% central (the least central collisions) and ending with bin 10 being 0-1% central (the most central collisions). The centrality of the collisions was determined by finding the number of particle tracks indicated by the detector for the range $-0.5 > \eta > 0.5$ which is the range of angles on the longitudinal plane for which the detector can trace the path of the particles.

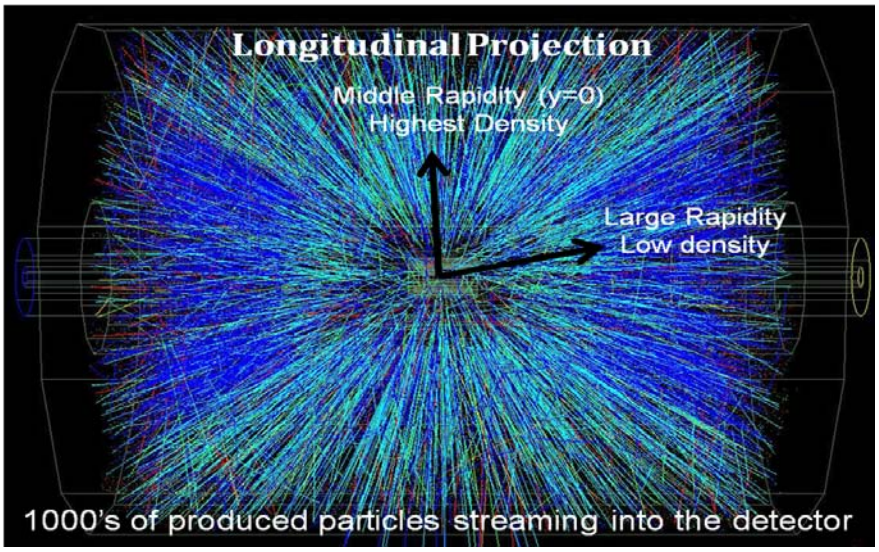

Figure 2: A model of the resulting particles on the longitudinal axis [STAR collaboration], Brookhaven National Laboratory

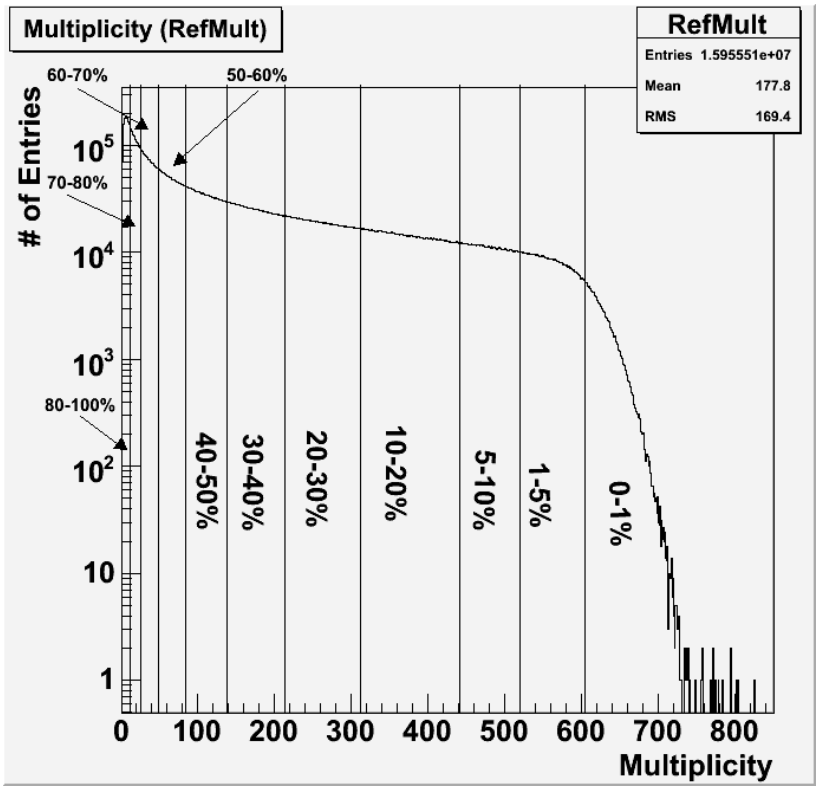

Figure 3: The graph of the number of entries vs. the multiplicity, which is the number of detected tracks

From this graph, projections or "cuts" were made of each centrality bin forming a graph of V_n^2 vs. $\Delta\eta$ for each values of n from 1 to 5, and for each centrality bin as shown in Figure 3. Gaussian fits of each graph were made and decomposed into a narrow Gaussian, and a wide Gaussian in which the narrow Gaussian represents non-flow correlations and the wide represent, V_n^2. Gaussians fits were used to determine the amplitude and width of the V_n^2 values. Each graph had the effects of non-flow correlation included, which is shown in the formula $\langle\cos[n(\varphi 1-\varphi 2)]\rangle = \langle V_n^2\rangle + \delta_n$, where δ_n is the non-flow correlation(Bilandzic, Snellings, and Voloshin. 2011). The non-flow correlations can be considered "interference" since they include jet-scattering and Bose-Einstein correlations which increase the number of two-particle correlations inside the data retrieved from the detector. Graphs were then made with the values of the amplitude and width of V_n^2 vs. n, where n is the harmonic number, along with the non-flow correlation values. A Gaussian fit was applied to the graph to find the width of the Gaussian (σ_n). The disk radius of the system was found using the

formula: $\sigma_n = 7.22 r_{part}^{-0.916}$. The disk radius is considered to be proportional to the mean-free-path of the particles.

Results

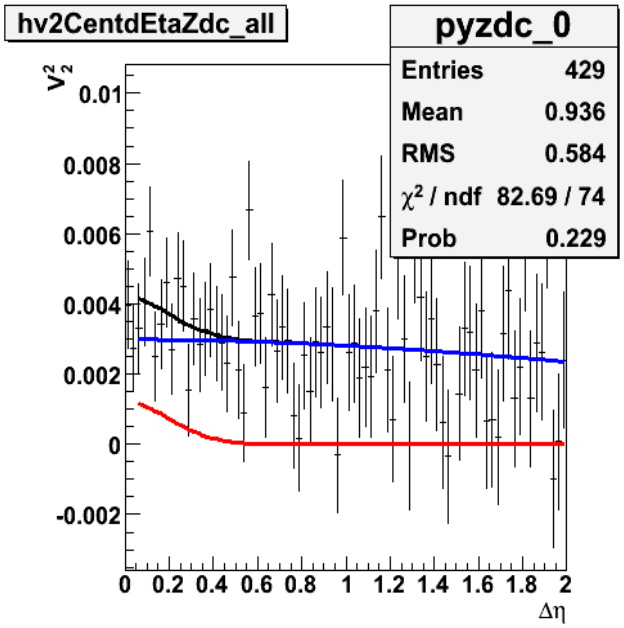

Figure 4: The Gaussian fit for the V_2 harmonic in centrality bin 0

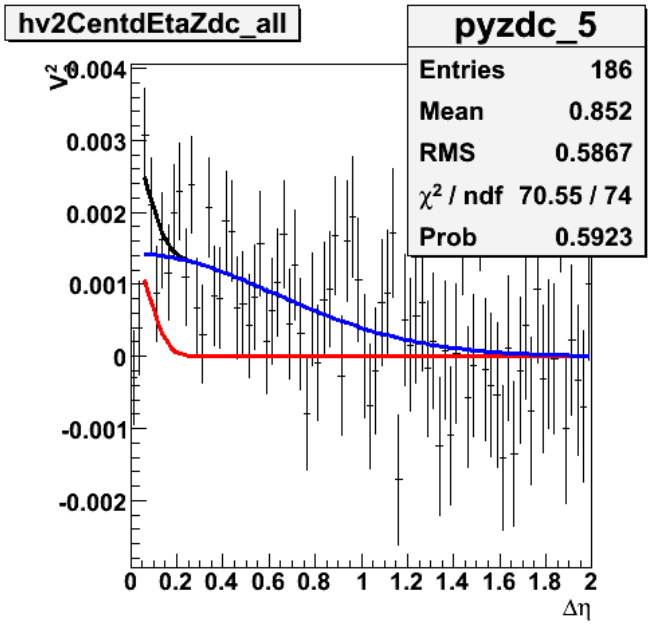

Figure 5: The Gaussian fit for the V_2 harmonic in centrality bin 5

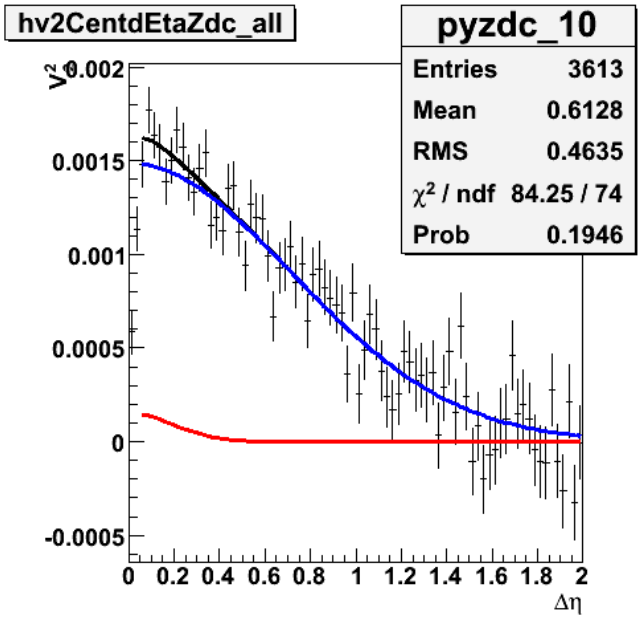

Figure 6: The Gaussian fit for the V_2 harmonic in centrality bin 10

Figures 4, 5, and 6 indicate how the amplitude and width of the Gaussian fits change along with the centrality of the collisions for V_2. The bottom curves with the small peaks are non-flow correlations which are removed from the graphs as corrections. The top curve is the uncorrected Gaussian fit, and the middle curve is the corrected Gaussian fit. The number of entries is the number of two-particle correlations, which reflects the particle

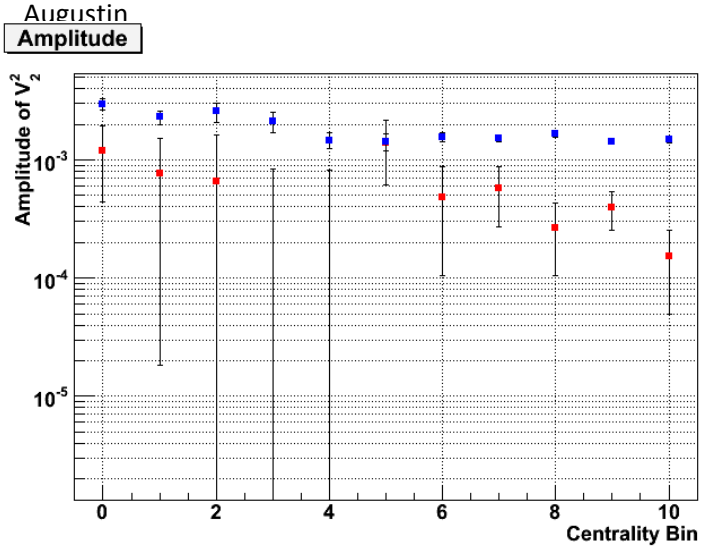

Figure 7: The plot of Gaussian amplitudes for each centrality bin for the V_2 harmonic

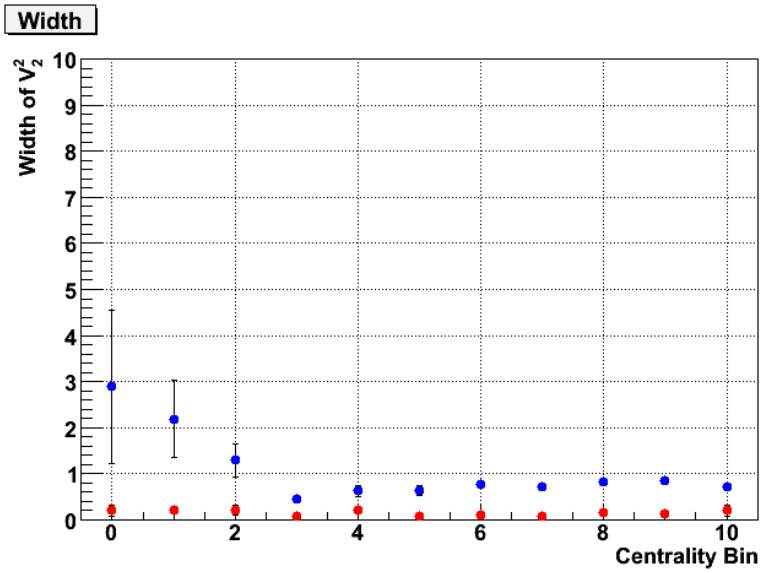

Figure 8: The plot of Gaussian widths for each centrality bin for the V_2 harmonic

yield relative to the centrality of the collisions. The less central collisions generally yield less particles and have higher error bars compared to the more central collisions.

Figures 7 and 8 compare the values of the amplitudes and widths of the Gaussian fit for each centrality bin. The general trend is that the amplitude increases with more central collisions; most likely there are fewer particles with increasing Δη because of the improbability of particles moving at that angle to each other with increasing centrality.

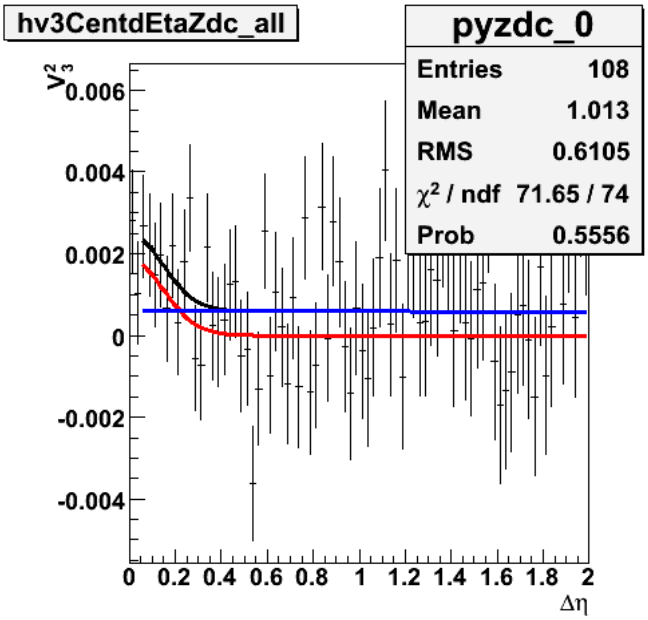

Figure 9: The Gaussian fit for the V_3 harmonic in centrality bin 0

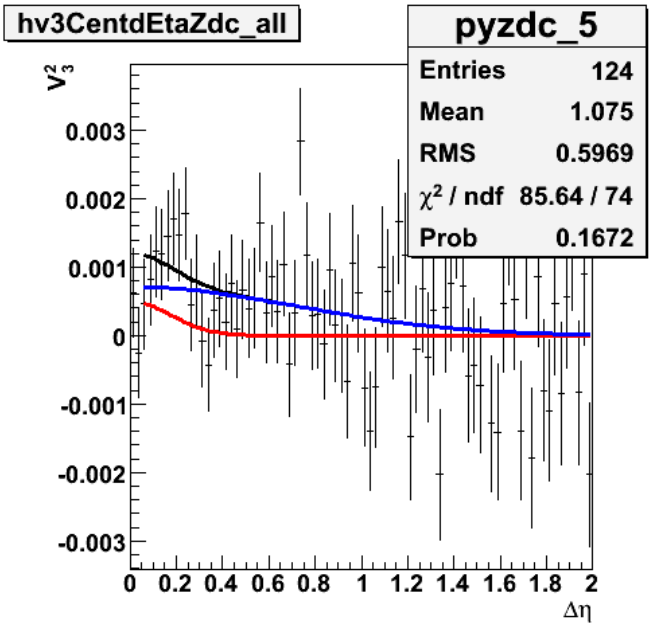

Figure 10: The Gaussian fit for the V_3 harmonic in centrality bin 5

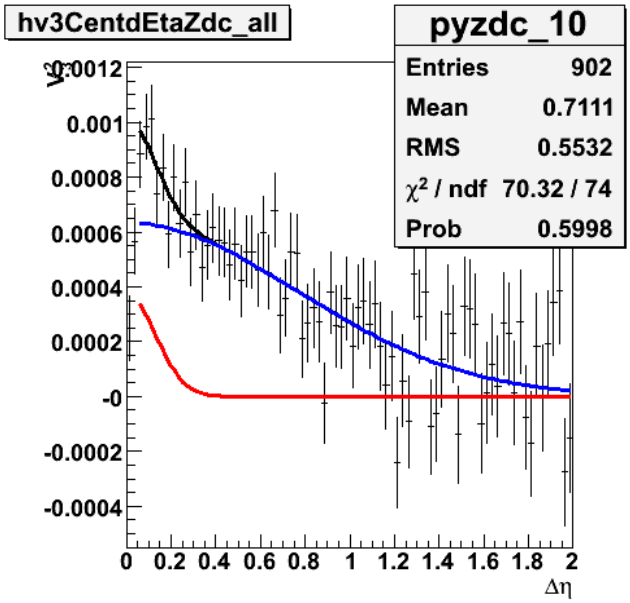

Figure 11: The Gaussian fit for the V_3 harmonic in centrality bin 10

Figures 9-13 are essentially created through the same processes as used for Figures 1-5, but for the V_3 harmonic. These differ from V_2 because of the shape they represent and the sheer difference in amplitude.

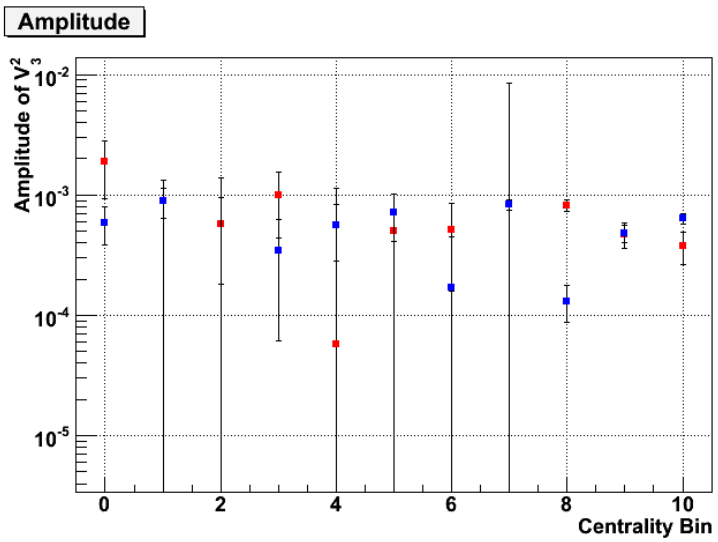

Figure 12: The plot of Gaussian amplitudes for each centrality bin for the V_3 harmonic

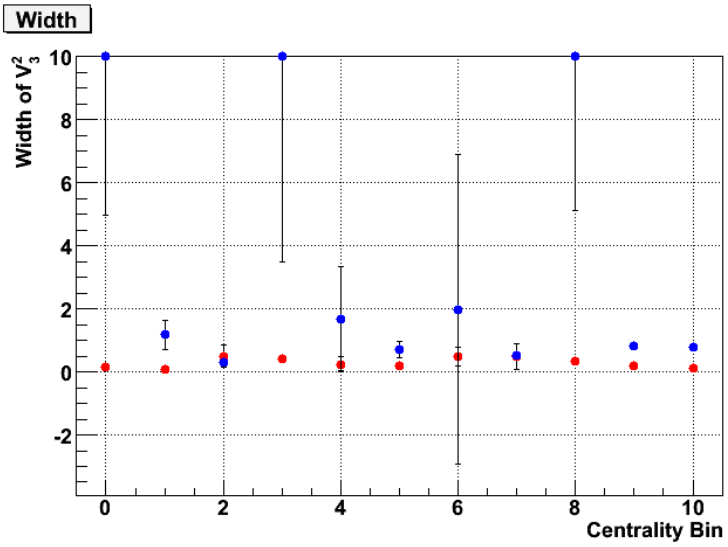

Figure 13: The plot of Gaussian widths for each centrality bin for the V_3 harmonic

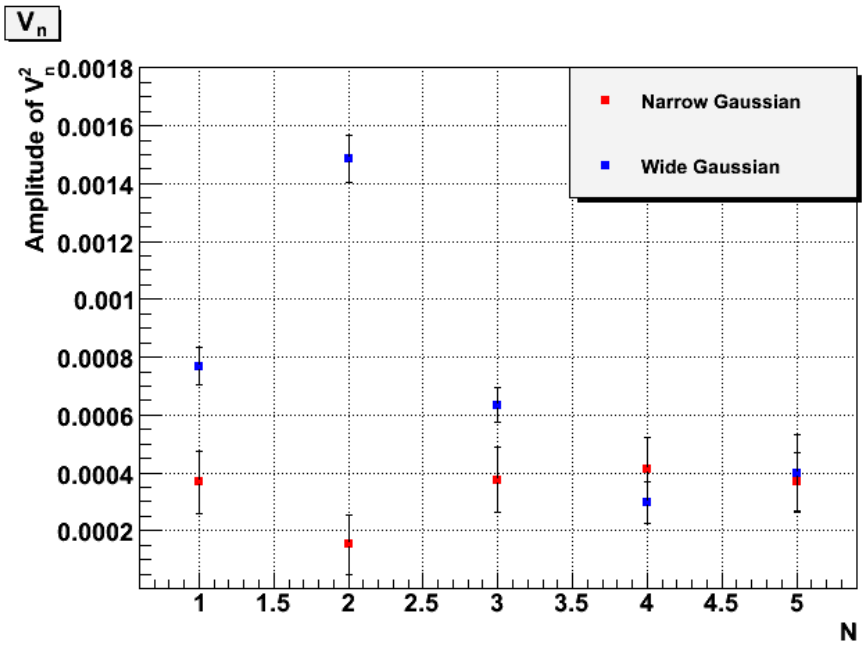

Figure 14: The plot of the Gaussian amplitudes against the harmonic number for centrality bin 10

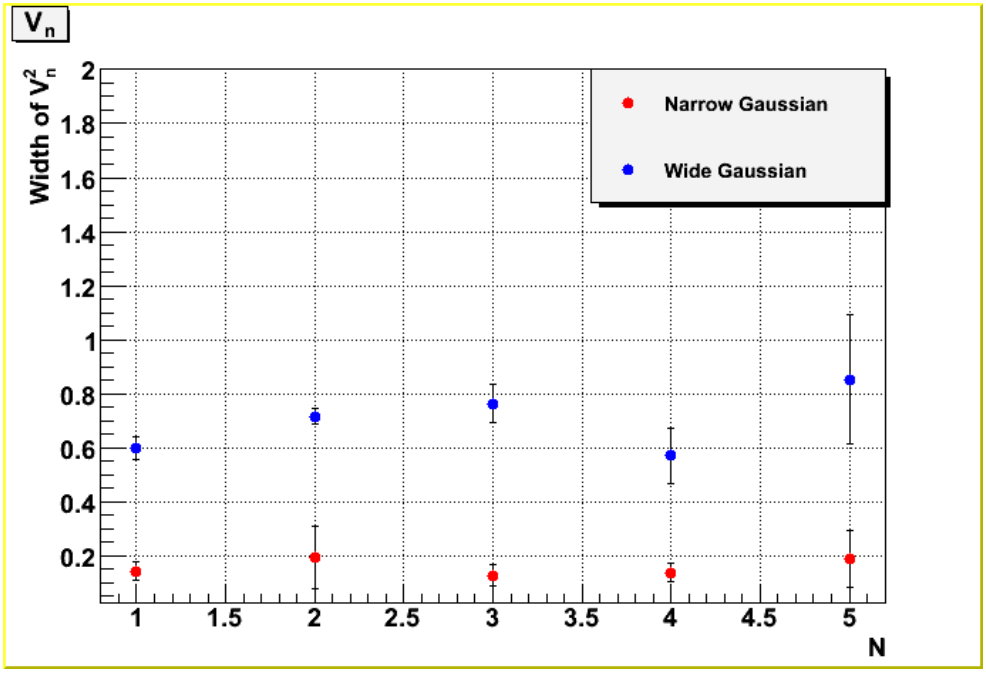

Figure 15: The plot of the Gaussian widths against the harmonic number for centrality bin 10

The figure 14 shows the inequalities of the amplitudes of each harmonic compared to each other, indicating that V_2 has a greater effect on the Fourier cosine series. The higher value V_2 indicates that the system has a almond-shape because it would have the shape of the cos(2ϕ) graph. The fact that the other harmonics do not equal zero show the density inhomogenities, meaning that the system reflects the shape portrayed by the other harmonic values. Figure 15 compares the widths of the harmonics showing how relatively flat they are. At the bottom of these graphs is the narrow Gaussian that represents non-flow correlation and at the top is the wide (corrected) Gaussian.

Figure 16 is used to find r_{part}, which is assumed to be equal to the mean-free-path (l_{mfp}). The Gaussian width (σ_n) is found from this plot of the amplitudes of each of the harmonics values for centrality bin 10. Because the higher harmonics seem to be approaching zero and r_{part} is not zero, these higher harmonics should be "washing out" due to viscous effects, thus indicating that viscous effects are present, so the viscosity of QGP is not zero. This washing out effect is demonstrated in figure 17. The value V_n^2 is directly proportional with the value of eccentricity, ε_n^2 which was graphed against n. As shown, r_{part} increases in value, ε_n^2 at higher harmonics are suppressed (Sorensen et al., 2011).

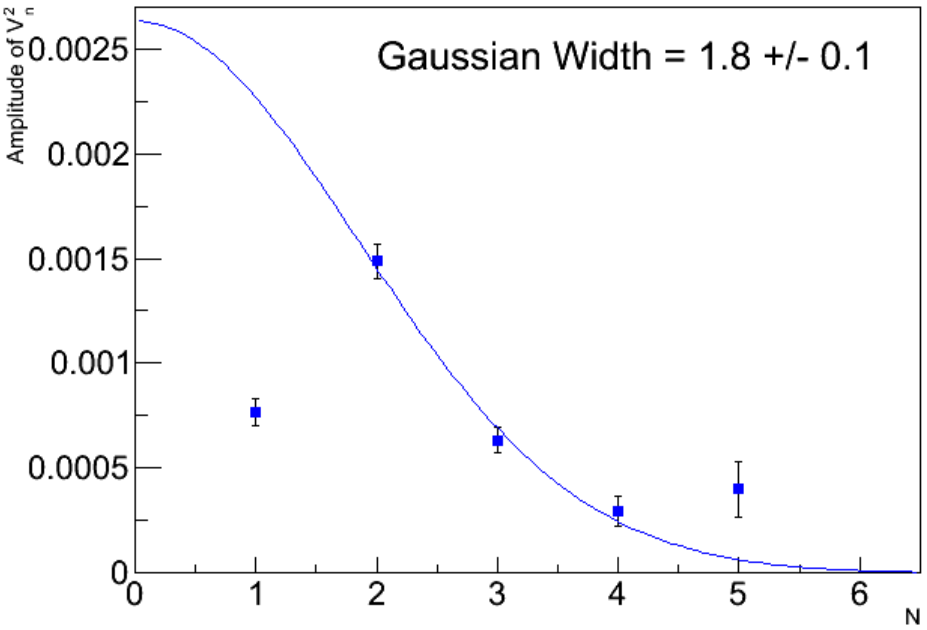

Figure 16: The Gaussian fit for the plots of amplitudes for each harmonic in centrality bin 10

$$\sigma_n = 7.22 r_{part}^{-0.916}$$

σ_n=1.83548 ± .110516

r_{part} ~ 4.45996 fm

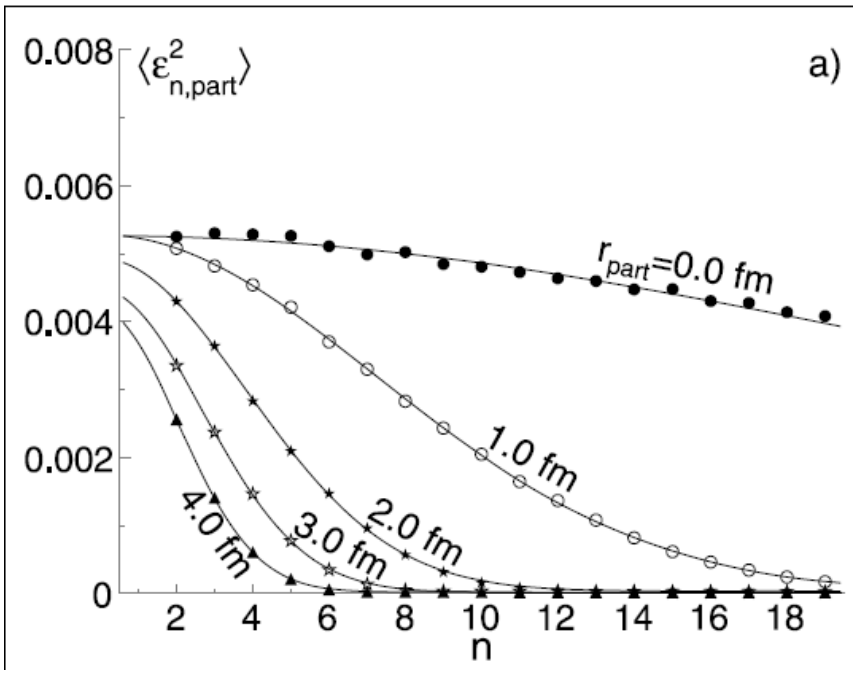

Figure 17: The Gaussian fits for eccentricity, ε_n^2 vs. harmonic value and the changes for r_{part}. (Sorensen et al. 2011)

Discussion

One of the many difficulties in this experiment is the fact that the formula, $\sigma_n = 7.22 r_{part}^{-0.916}$, is derived from the relationship of ε_n^2 to n, with the assumption that V_n^2 is proportional to but not equal to ε_n^2. The validity of the equation itself is still debatable, at least in the case of using the width of the Gaussian fits of the V_n^2 values. Further analysis is needed to determine how the error of the Gaussian width, σ_n, will affect the value of r_{part}. Since l_{mfp} and r_{part} are equivalent, and since l_{mfp} is related to viscosity, the value of r_{part} reveals clues about the viscosity of QGP. As of yet, no such method exists to yield viscosity from a value of l_{mfp} currently available, so only the presence of viscosity can be indicated, but not its exact value.

In the graphs for V_n^2 vs. $\Delta\eta$ (Figures 4-6, 9-11), the non-flow correlation is corrected for, since the non-flow correlation increases the number of two-particle correlations, interfering with the Gaussian fit at low values of $\Delta\eta$. The amplitude of V_2^2 is greater than the other harmonics. These results indicate that viscosity is not as small as was expected since the size of V_2^2 affects the Gaussian fit that is used to determine r_{part}, and r_{part}, in turn, reflects viscosity.

The question still remains as to how to measure quantifiably the viscosity of the QGP. It is a question that particle physicists will continue to study through analysis of particle collisions. One possible step to better quantifying the viscosity of QGP would be to collide a variety of subatomic particles at high energies, calculate the mean-free-path for each type of collision, and compare results. Defining the relationship between viscosity and the mean-free-path will lead to a better understanding if the QGP, and ultimately the nature of the Big Bang.

References

1) Bilandzic, Ante, Raimond Snellings, and Sergei Voloshin. "Flow analysis with cumulants: Direct calculations." *Physical Review C* 83.044913 (2011): n. page. Print.

2) Jacak, Barbara, and Peter Steinburg. "Creating the perfect liquid in heavy-ion collisions." *Physics Today* May 2010: 39-43. Print.

3) Sorensen, P., et al. "The rise and fall of the ridge in heavy ion collisions." *Physics Latter B* 705 (Nov. 2011): 71-75. Print.

4) Trafton, Anne. "Explained: Quark-gluon plasma." *MIT news*. Massachusetts Institute of Technology, 9 June 2010. Web. 29 July 2011. <http://web.mit.edu/newsoffice/2010/exp-quark-gluon-0609.html>.